

ORIGINAL RESEARCH

## Regeneration of dentine/pulp-like tissue using a dental pulp stem cell/poly(lactic-co-glycolic) acid scaffold construct in New Zealand white rabbits

Rania M. El-Backly, BDS, MS<sup>1</sup>; Ahmed G. Massoud, BDS, MS, PhD<sup>2</sup>; Azza M. El-Badry, BDS, MS, PhD<sup>3</sup>; Raef A. Sherif, BDS, MS, PhD<sup>2</sup>; and Mona K. Marei, BDS, MS, PhD<sup>4</sup>

1 Department of Conservative Dentistry-Endodontics Branch, Tissue Engineering, Laboratories, Faculty of Dentistry, Alexandria University, Alexandria, Egypt

2 Department of Conservative Dentistry-Endodontics Branch, Faculty of Dentistry, Alexandria University, Alexandria, Egypt

3 Department of Oral Biology, Faculty of Dentistry, Alexandria University, Alexandria, Egypt

4 Tissue Engineering Laboratories, Faculty of Dentistry, Alexandria University, Alexandria, Egypt

### Keywords

cell/scaffold construct, dental pulp stem cells, dentine/pulp-like tissue, regenerative endodontics, tissue engineering.

### Correspondence

Ms Rania M. El-Backly, 9 Al-Ekbal St., Victoria, Alexandria 21411, Egypt. Email: raniaoaman@gmail.com

doi:10.1111/j.1747-4477.2008.00139.x

### Abstract

With the expanding knowledge of tooth regeneration and biological mechanisms of functional dental tissue repair, current treatment strategies are beginning to give way to evolving fields such as tissue engineering and biomimetics. Dental pulp stem cells were isolated from rabbit teeth and seeded onto scaffolds prepared from 50/50 poly(lactic-co-glycolic acid) polymers using two different porogen particle sizes. These cell/scaffold constructs were then transplanted subcutaneously in the rabbits. The expanded rabbit dental pulp stem cells showed high proliferative and clonogenic capacities as well as the ability to give rise to mineralised-like tissues *in vitro* in culture flasks and after seeding them onto the scaffolds for 12 days. Histological evaluation of transplanted samples revealed the formation of osteodentine-like structures as well as tubular bilayered structures of vertically aligned parallel tubules resembling tubular-like dentine. Using a tissue engineering approach yielded tissues quite similar to normal dentine/pulp-like tissues that can perhaps be used later on for regenerative endodontic or operative procedures.

### Introduction

Over the past century, endodontic therapy has shown a high rate of success in retention of teeth; however, this is not always possible. Many teeth remain unrestorable due to several reasons, and vital pulp therapy procedures are not always predictable, often resulting in the need for eventual endodontic therapy (1).

In view of the increasing demand for maintaining pulp vitality and the high cost of endodontic treatments being performed every day, there has been increasing interest in investigating new methods for tissue replacement (2). With the expanding knowledge of developmental biological processes, and how they are mimicked during dental tissue repair, strategies to regenerate lost or diseased dental tissue will soon enter into clinical practice (3).

Tissue engineering involves the development of functional tissue with the ability to replace missing or damaged tissue. This may be achieved either by transplanting cells seeded into a porous material or scaffold having open pores or by relying on ingrowth of cells into such a material, which in both cases develops into normal tissue (4,5).

It has been consistently shown that the dental pulp contains cells that can differentiate into hard tissue forming cells following injury. Damaged odontoblasts can be replaced by newly regenerated populations of odontoblast-like cells derived from stem cells residing in the dental pulp. Cell therapy utilising dental pulp stem cells has the potential to improve conventional pulp capping with artificial materials that can induce only a small amount of replacement dentine beneath the exposed or amputated site of the pulp (6).

Numerous reports have identified and successfully isolated a highly proliferative and clonogenic population of stem cells from the dental pulp (7–9). These cells have shown the ability to differentiate into odontoblasts and regenerate dentine/pulp tissue resembling normal physiologic tissue (10,11).

Most of these reports have focused on the putative regenerative potential of this population of dental pulp stem cells; however, information regarding the nature of the scaffold or carrier for this specific tissue remains lacking. Structurally, the dental/pulp complex differs from all other specialised tissues of the body regarding its inherent architectural arrangement and the functional harmony of these two different tissues: dentine and pulp (12).

In the current work, we hypothesised the use of 50/50 poly(lactic-co-glycolic acid) (PLG) scaffolds with different porosities co-cultured with rabbit dental pulp stem cells (RDPSCs) and transplanting them subcutaneously to evaluate the potential of this stem cell/scaffold construct to regenerate dentine/pulp tissue. We also focused on exploring the nature of the regenerated tissues for potential use of this therapy for regenerative endodontic procedures. To our knowledge, this is the first documentation of successful isolation and characterisation of dental pulp stem cells from New Zealand white rabbit teeth.

## Materials and methods

### Preparation of biodegradable polymer sheet scaffolds

Biodegradable polymer sheet-form scaffolds were fabricated using the solvent casting/particulate leaching technique (13,14) from Synthetic biodegradable 50/50 poly(DL-Lactide-CO-Glycolide) '50/50 DL-PLG' with inherent viscosity 0.57 dL g<sup>-1</sup> in HFIP at 30°C (Absorbable Polymers International, Pelham, AL, USA). Briefly, Sodium Chloride (Sigma Aldrich, St. Louis, MO, USA) (the salt porogen) is mixed with a solution of 10 mL of chloroform (Fluka/Chemika 25691, Buchs, Switzerland) in which 1 gm of the polymer (50/50 DL-PLG) has previously been dissolved and then the solution is cast into a 5-cm Petri dish and left overnight for the chloroform to evaporate. This yields uniform sheets which are then subjected to a leaching procedure so that all the salt is leached out leaving pores.

These sheets are then freeze-dried to achieve partial dehydration and to completely eliminate moisture from the sheets. A total of 90% (0.9 gm) weight fraction of salt was used, that is, polymer/porogen ratio was 1 gm : 0.9 gm, with two different particle sizes, 150–180 µm and 180–300 µm achieved by sieving in an

automatic sieve shaker. This procedure gave rise to two groups: group I polymer sheet scaffolds with 90% weight fraction of salt 150–180 µm particle size, and group II polymer sheet scaffolds with 90% weight fraction of salt 180–300 µm particle size. The sheets were then divided into 2 × 2 mm<sup>2</sup> pieces.

### Scanning electron microscopy and mercury intrusion porosimetry characterisation of prepared scaffolds

The prepared scaffolds were subjected to scanning electron microscopy (SEM; Jeol, Tokyo, Japan) to evaluate pore size, porosity and pore interconnectivity as well as surface morphology and topography. The samples were subjected to dehydration procedures prior to coating with gold for 2 min using a sputter coater. Mercury intrusion porosimetry allows data to be acquired over a broad dynamic range using a single theoretical model. Mercury porosimetry routinely is applied over a capillary diameter ranged from 0.003 µm to 360 µm. Not only is mercury porosimetry applicable over a wide range of pore sizes, but also the fundamental data it produces (the volume of mercury intruded into the sample as a function of applied pressure) are indicative of various characteristics of the pore space and are used to reveal a variety of physical properties of the solid material itself (15). For the mercury intrusion porosimetry measurements (Poresizer 9320 V2.08) (ASTM: D2873 Micrometrics, Norcross, GA, USA), samples were weighed and penetration volume readings were obtained starting from 1.19 to 1.29 psia where pore diameters ranging from 141 to 152 µm were filled with mercury. Recordings were made until the pressure reached 29 985 psia where 0.0060-µm diameter pores were filled with mercury.

### Isolation and characterisation of RDPSCs

Dental pulp stem cells were isolated from four New Zealand white rabbits. All the rabbits used for this study were males, 3–4 weeks old, and with an average weight of 2–3 kg. All experimental animal procedures were carried out based on the NIH guidelines for the care and use of laboratory animals. For extirpation of healthy pulp tissue, general anaesthesia was administered using Xylazine HCL 2% in a dose of 20 mg kg<sup>-1</sup> body weight followed by ketamine HCL in a dose of 100 mg kg<sup>-1</sup> body weight intra-peritoneal. From each rabbit one of the sound lower incisors was extracted gently to avoid root fracture. The tooth was cleaned, then placed in a 50-mL falcon tube containing a 5-mL sterile solution of antibiotics for 5–10 min.

Cell culture procedures were then followed to isolate dental pulp stem cells (7–10). The pulp tissue was

dissected from inside of the crown and root of the tooth using sterile files, reamers and excavator. The pulp tissue was then placed in supplemented cell culture media containing: Dulbecco's modified Eagle's medium (DMEM) or alpha modification of Eagle's medium ( $\alpha$ -MEM) (Cambrex, Charles City, IA, USA), containing: 20% fetal bovine serum (Cambrex), 1% L-glutamine (Cambrex), 1% penicillin (10 000IU) – streptomycin (10 000  $\mu$ g) (Cambrex), 2% Hepes buffer (Cambrex) and 50  $\mu$ g ml<sup>-1</sup> L-ascorbic acid (GIBCO, Carlshad, CA, USA).

The pulp tissue was then dissected into 2 × 2 mm<sup>2</sup> pieces, washed in phosphate buffered saline (PBS) (Cambrex), then incubated in 3 mg mL<sup>-1</sup> collagenase type I (GIBCO) and 4 mg mL<sup>-1</sup> dispase (GIBCO) for 1 h in the CO<sub>2</sub> incubator at 37°C, 5% CO<sub>2</sub> and 95% humidity. Single cell suspensions were then obtained and cultured in 75 cm<sup>2</sup> tissue culture flasks in supplemented media, and placed in the CO<sub>2</sub> incubator (37°C, 5% CO<sub>2</sub> and 95% humidity). Day 14 cultures were tested for colony-forming efficiency using Toluidine Blue (GIBCO). At 80% confluence, cells were subcultured, counted and tested for viability using the Trypan blue dye exclusion test. Second or third passage RDPScs were used for all subsequent experiments.

For characterisation of RDPScs, the monoclonal antibody p75 NGF receptor (NGFR5) (cd271) mouse anti-rabbit (Abcam, Cambridge, MA, USA) was used as the primary antibody and fluorescein labelled antisera rabbit anti-mouse IgG1 (Antibodies Incorporated, Davis, CA, USA) was used as the secondary antibody. Samples were viewed using a Confocal Laser microscope (BIORAD, Segrate, Italy).

#### Culturing RDPScs onto prepared biodegradable porous scaffold sheets

This step was done 2–3 days prior to transplantation subcutaneously in the dorsal surface (back) of the rabbit. Scaffolds were divided into two main groups for each of the two groups of scaffolds prepared. One group represented the control samples which received no cells and the other group represented the experimental samples which were seeded with RDPScs. Scaffolds were sterilised by soaking in absolute ethyl alcohol for 30 min. Sheets were then thoroughly rinsed with PBS for 1 h. Supplemented media were then added for 30 min to 1 h. Control scaffolds received cell culture media alone (1-mL medium/well, and 4–6 sheets/well), and were placed in the CO<sub>2</sub> incubator (5% CO<sub>2</sub>, 37°C and 95% humidity).

For the experimental group which received cells, second or third passage RDPScs were used for seeding of the scaffolds for all of the groups. Seeding densities ranged from 0.5 × 10<sup>6</sup> to 1 × 10<sup>6</sup> cells mL<sup>-1</sup> and the seeded

scaffolds were placed in the incubator and left overnight. The following day, the plates were removed and the scaffolds inverted on the other side, to ensure complete seeding on both surfaces of the scaffold. The media were aspirated, a new cell suspension added, and again left overnight. The next day, the cell suspension was aspirated to remove any non-adherent cells and fresh medium was added. Scaffolds were placed in the incubator till the time of surgery.

Following seeding procedures, cell/scaffold constructs were evaluated from 1 to 12 days post-seeding using the inverted phase contrast microscope (NIKON, Tokyo, Japan) and SEM to evaluate cell attachment and proliferation onto the scaffolds. Prior to SEM evaluation, cell/scaffold constructs were first fixed using a solution of Glutaraldehyde (25%) (SIGMA, St Louis, MO, USA), Formalin (10%) (SIGMA), sodium hydroxide (SIGMA), sodium monophosphate (SIGMA) and distilled water for 24 h at 4°C, then subjected to dehydration and coating.

#### Subcutaneous transplantation of seeded and unseeded scaffolds

All the animals in this stage received constructs consisting of their own previously expanded cells (autogenous). The animals were divided into two groups, group I which received group I scaffolds [(0.9 gm) weight fraction of salt, 150- to 180- $\mu$ m particle size] (control: cultured in medium alone, and test: cultured with RDPScs) and group II [(0.9 gm) weight fraction of salt, 180- to 300- $\mu$ m particle size] which received group II scaffolds (control: cultured in medium alone, and test: cultured with RDPScs). There were two rabbits per group; each received four samples: two control samples and two test samples (Table 1).

General anaesthesia was administered using Xylazine HCL 2% in a dose of 20 mg kg<sup>-1</sup> body weight followed by ketamine HCL in a dose of 100 mg kg<sup>-1</sup> body weight intra-peritoneal. For each rabbit, four subcutaneous pouches were created on the dorsal surface of the rabbit, by blunt dissection, with a distance of approximately 2 cm in between pouches. The pouch created was made so as just to encompass the sheet scaffold and was not deep to maintain the underlying fascia intact. The control samples were placed in the two right pouches and the test samples were then placed in the two left pouches. The subcutaneous pouches were then sutured using 3.0 silk suture material.

At 2 and 6 weeks, full thickness sections with the samples from both control and test groups were removed, and immediately placed in 10% formalin fixative. Histological sections were then obtained and stained with haematoxylin and eosin.

**Table 1** Experimental animal groups and number of samples

Group #	Group I		Group II	
	Control (without cells)	Test (seeded with RDPSCs)	Control (without cells)	Test (seeded with RDPSCs)
Type of sample (control or test)				
No. of samples	4	4	4	4
No. of samples retrieved after 2 weeks	2	2	2	2
No. of samples retrieved after 6 weeks	2	2	2	2

RDPSCs, rabbit dental pulp stem cells.

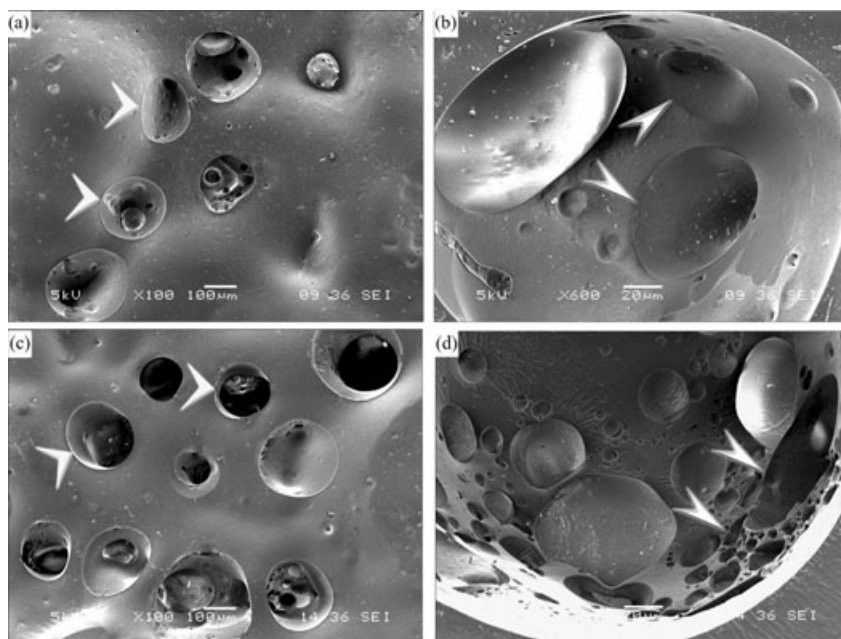


**Figure 1** Scanning electron micrographs for 50/50 PLGA scaffolds. (a,b) SEM for group I scaffolds ( $\times 100$  and  $\times 600$  respectively) showing surface topography and pore distribution in (a). Higher magnification in (b) shows interconnecting pores, (c,d) SEM for group II scaffolds ( $\times 100$  and  $\times 600$  respectively) showing surface topography and increased pore distribution in (c) than for group I. Higher magnification in (d) shows numerous interconnecting pores within one of the large surface pores.

## Results

### Scanning electron microscopy and mercury intrusion porosimetry assessment of prepared scaffolds

For group I, containing 0.9-gm salt with particle size 150–180  $\mu\text{m}$ , the size of the pores ranged from 8 to 250  $\mu\text{m}$  with numerous pores of the smaller scale (Fig. 1a). Interconnectivity was also revealed for the larger pores showing interconnecting pores that reached 160  $\mu\text{m}$  in size (Fig. 1b). As for group II, using 0.9-gm salt with particle size 180–300  $\mu\text{m}$ , the pore sizes ranged from 30 to more than 300  $\mu\text{m}$  (Fig. 1c). Most of these surface pores lay in the range of 100  $\mu\text{m}$ . Higher magnifications also revealed excellent pore interconnectivity with pores ranging from 3 to almost 70  $\mu\text{m}$  in size (Fig. 1d).

Mercury porosimetry measurements were performed for samples from each group. The results were plotted in the form of several graphs. The most significant of which are the plots of incremental intrusion versus diameter. The graph represents the variety of pore diameters filled by mercury for each group. Macropores, mesopores and micropores are represented on the graph.

For group I (0.9-gm salt, 150- to 180- $\mu\text{m}$  pore size), the total pore area represented was 71.208  $\text{m}^2 \text{g}^{-1}$ . Median pore diameter (volume) was 0.0986  $\mu\text{m}$ . This group recorded a porosity percentage of 37.02%. On the graph representing incremental intrusion versus diameter of pores, both macropores and micropores were represented well on the graph; however, mesopores were few (Fig. 2a). As for group II (0.9-gm salt, 180- to 300- $\mu\text{m}$  pore size), total pore area was 43.466  $\text{m}^2 \text{g}^{-1}$  and median

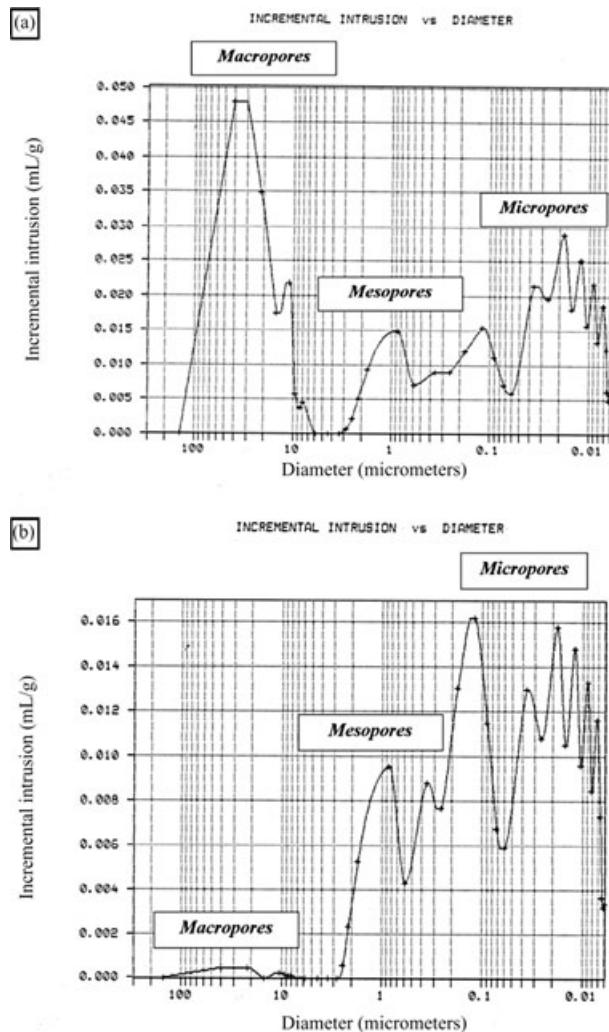


**Figure 2** Graphs representing incremental intrusion versus diameter showing the distribution of different pore sizes throughout the scaffold where macro-, meso- and micropores are represented on the graphs for (a) group I showing high distribution of mainly macropores, and (b) group II showing most of the pores to be micropores.

pore diameter (volume) was  $0.0324 \mu\text{m}$ . As for the porosity percentage, this group recorded porosity at 20.56%. On the graph representing incremental intrusion versus diameter, micropores were the dominating kind as well as the mesopores. As for macropores, those were very few (Fig. 2b).

#### Isolation and characterisation of RDPSCs

Dental pulp stem cells were successfully isolated from the pulps of rabbit teeth. The cells began to attach to the bottom of the flasks, and hence appeared with various morphologies, some spindle-like and others appeared

stellate-shaped, while many appeared polygonal, thus reflecting the diversity of the morphology of stem cells. By day 3, cells had begun to form colonies which could be identified in many areas of the flask. The cells continued to proliferate and propagate as colonies until 80% of the flask area was covered with cells by day 14, indicating a highly clonogenic and proliferative cell population in the dental pulp. Following confluence, the cells were successfully passaged (Fig. 3a,b).

During the primary culture as well as in the first and occasionally second passages, the dental pulp stem cells seemed to form very well-condensed colonies. By time, these colonies matured and the cells appeared to secrete a dense extracellular matrix which matured by day 26 in the form of concentric circles with a well-defined centre, after which they became visible to the naked eye. Upon fixation and staining with haematoxylin and eosin, these structures appeared as dark eosinophilic circles distributed in several areas of the flask. Furthermore, when these colonies were left in culture up until day 67, the dense extracellular matrix secreted appeared to extend tubule-like extensions (Fig. 3c-f). RDPSCs revealed 96% viability and a colony-forming efficiency of approximately 47–53 colonies per  $10^4$  cells (initial plating density).

Immunophenotyping of isolated and cultured RDPSCs revealed their immunoreactivity when treated with the marker p75 nerve growth factor receptor 5 (CD271). Immunoreactivity was demonstrated in experimental specimens that received both primary and secondary antibodies (Fig. 3h) but not in the control specimens which received only the secondary antibodies (Fig. 3g).

#### Culturing RDPSCs onto prepared biodegradable porous scaffold sheets

Phase contrast micrographs for group I samples showed surface pores in the scaffolds with a density of cell attachment and proliferation in and around these pores throughout the experiment period. Degradation was apparent by the erosion of pore margins and increased porosity (Fig. 4a). For group II, phase contrast micrographs were similar to those of the previous group, yet surface porosity was not that apparent (Fig. 4b).

Group I scanning electron micrographs showed cell attachment in day 5 seeded samples with cell processes bridging the pores. Day 12 seeded samples showed obvious progress with the presence of several nodule-like structures on the surface. Looking closely at the day 12 seeded samples, these nodule-like structures had become much more organised and more densely packed together appearing similar to nidi of mineralisation (Fig. 5a). Scanning electron micrographs of group II scaffolds showed at

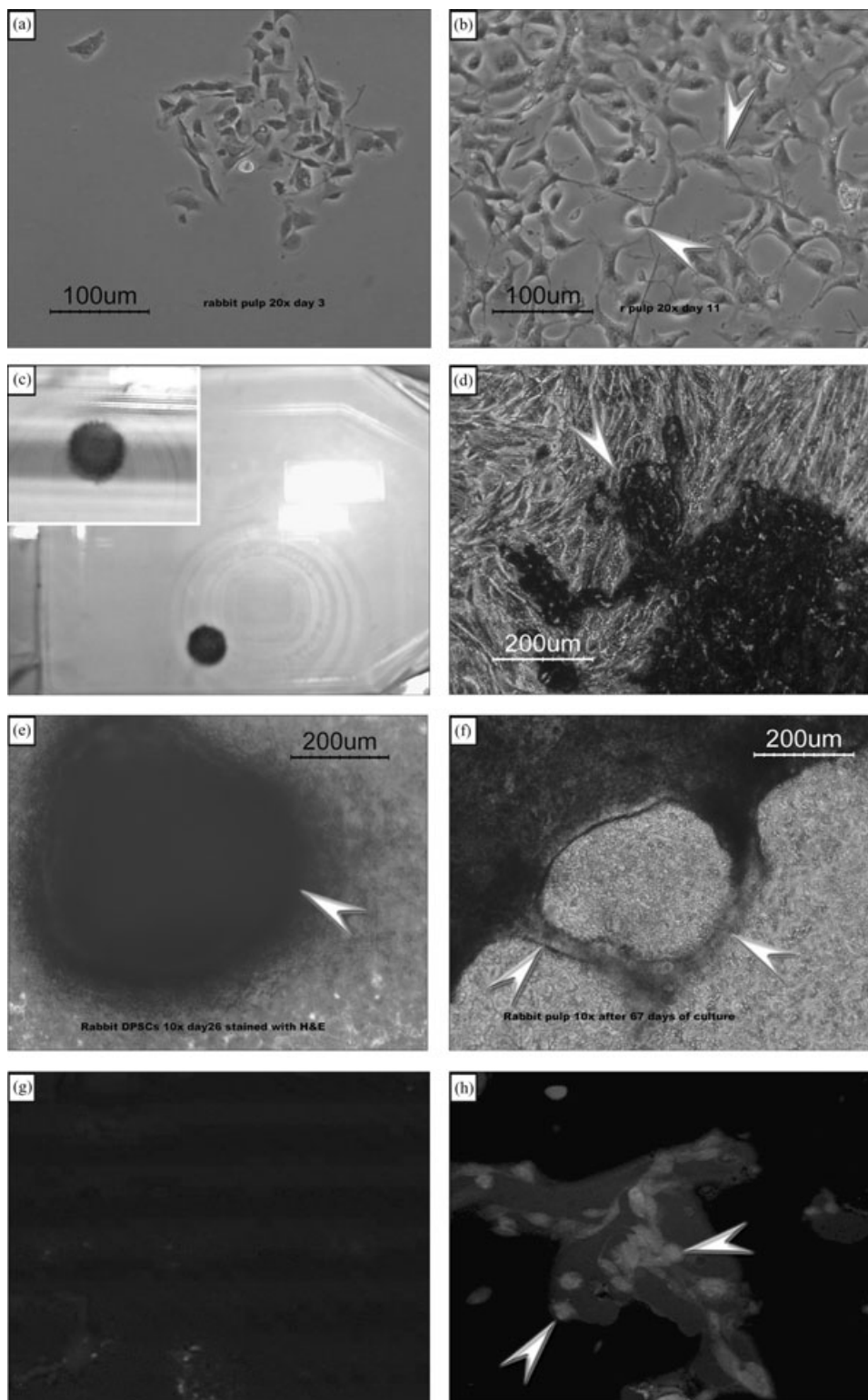


**Figure 3** Cell proliferation and colony formation in culture of dental pulp stem cells. (a,b) Dental pulp stem cells in culture, days 3 and 11 respectively ( $\times 200$ ); (c) staining of nodules by H&E ( $\times 100$ ); (d) phase contrast micrograph showing stained cells and matrix ( $\times 100$ ); (e) micrograph showing concentric lines in nodule stained with H&E ( $\times 100$ ); (f) day 67 cultured cells showing dense extracellular matrix with tubule-like extensions from it ( $\times 100$ ); (g,h) immunophenotyping using confocal laser microscopy and CD271 ( $\times 400$ ). Control samples in (g) stained with secondary antibody alone showing absence of reaction and test samples in (h) stained with primary and secondary antibodies showing positive immunoreactivity.

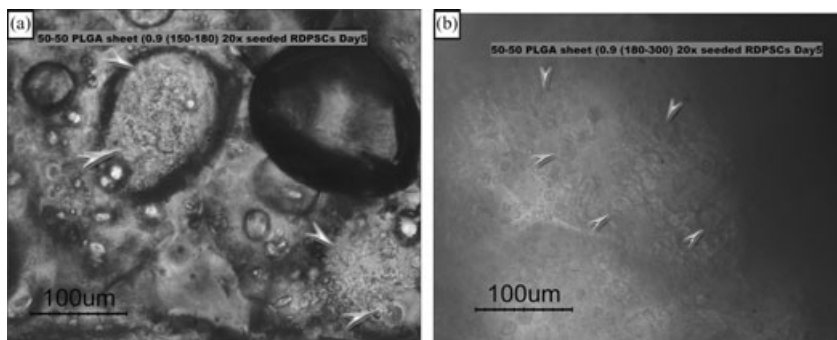


**Figure 4** Inverted phase contrast micrographs of groups I and II, 50/50 PLGA scaffolds seeded with rabbit dental pulp stem cells (RDPSCs) – day 5. (a) Group I scaffolds seeded with RDPSCs where cells are distributed throughout the pores of the scaffold (arrows); (b) group II scaffolds seeded with RDPSCs showing the cells proliferating on the entire surface area of the scaffold (arrows).

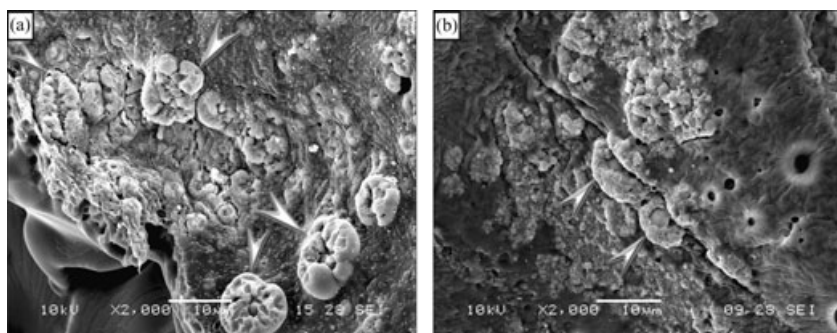


**Figure 5** Scanning electron micrographs of groups I and II scaffolds seeded with rabbit dental pulp stem cells – day 12. (a) Group I seeded scaffolds with rabbit dental pulp stem cells showing numerous nodule-like structures on surface of scaffold (arrows) (×2000); (b) group II seeded scaffolds with rabbit dental pulp stem cells showing dense extracellular matrix on surface and some nodule-like cell clusters (arrows) (×2000).

day 5, numerous cell colonies inside the surface pores and extending to infiltrate interconnecting pores as well. At day 10, the surface revealed numerous cells and dense extracellular matrix appearing in the form of a network covering the surface of the scaffold. Day 12 samples revealed many nodule-like clusters of cells dispersed unevenly along the surface of the scaffold. By day 12, the higher magnifications again revealed well-organised nodule-like structures densely packed together and interspersed with less organised extracellular matrix. Degradation of the surface was also evident by the appearance of more pores (Fig. 5b).

**Histological results of the subcutaneously transplanted seeded and unseeded scaffolds**

All specimens were viewed under the light microscope at the specified intervals and micrographs were taken for representative samples from every group. In general, at the time of retrieval of the samples, the dorsal skin appeared normal and hair had already begun to cover the

site of transplantation by 2 weeks and totally covered it by 6 weeks, for all control and test samples. When samples were dissected, there was an obvious increase in vascularity at the area of the transplants.

Upon histological examination of the specimens, there were no signs of inflammatory cells in any of the specimens for both groups at any of the intervals. The skin appeared completely healed with a continuity of the superficial epithelial layers and presence of normal skin appendages in all samples. There was also a noticeable increase in the number of blood vessels and budding capillaries in all of the specimens. However, this phenomenon was much more pronounced with the cell-seeded transplants than those that received the scaffold alone especially in the areas where characteristic regenerated tissues could be seen.

In the control (scaffold alone) 2-week samples for group I, there was a very dense fibrous scar tissue extending over a wide area and reaching up to the epidermis probably delineating the pathway of entry and the site of the transplant (Fig. 6a). Higher magnification of this

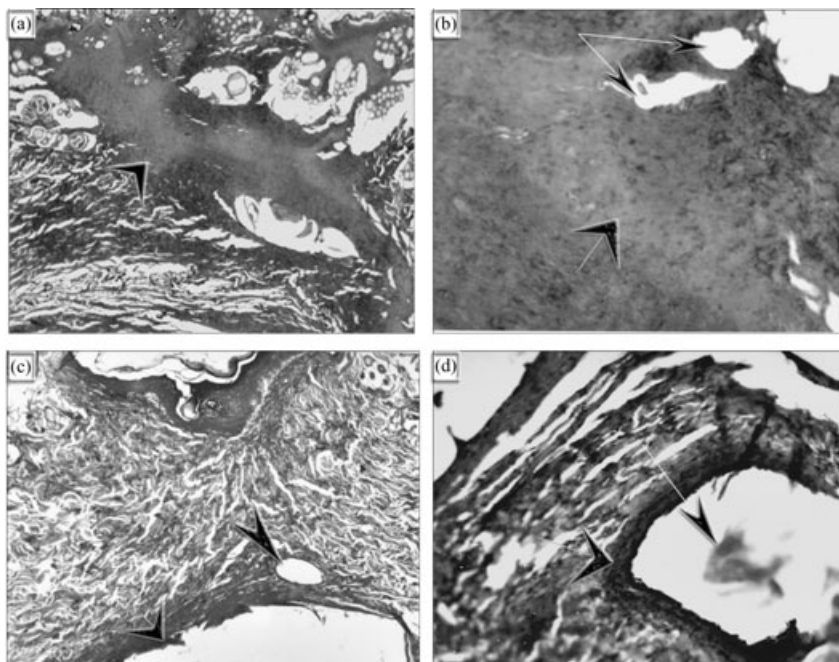


**Figure 6** Histological micrographs of group I implants – 2 weeks following transplantation (H&E). (a) Control sample (without cells) showing dense fibrous tissue at the site of wound entry ( $\times 40$ ); (b) control sample (without cells) showing dense fibrous tissue (wide arrowhead) and spaces (narrow arrowheads) left by scaffold ( $\times 200$ ); (c) test sample (with cells) showing a fibrous tissue capsule (wide arrowhead) containing spaces (narrow arrowhead) left by the degrading scaffold ( $\times 40$ ); (d) test sample (with cells) showing a structure with layers of well-organised cells (wide arrowhead) and a secretory-like product in its lumen (narrow arrowhead) ( $\times 200$ ).

dense tissue revealed a density of collagen fibres as well as the spaces left by the degrading scaffold (Fig. 6b).

In the 2-week test samples of group I, there was an obvious thickening of the epithelium over the area of wound entry (Fig. 6c). The underlying area contained dense collagen fibres and was devoid of skin appendages. Remnants of a fibrous tissue capsule could be seen above the muscle layer. Around this capsule there were large spaces which may have contained traces of the polymeric scaffold. A characteristic of this specimen is, the presence of a well-circumscribed structure related to the capsule wall lined by well-organised cells in several layers. Within the lumen of this structure, there is a secretory-like product (Fig. 6d).

For the group II 2-week control samples, there was a dense fibrous tissue capsule circumscribing the area of the transplant (Fig. 7a) and close to the wall of the capsule are numerous budding capillaries (Fig. 7b). For the group II 2-week test samples (cell/scaffold transplants), a fibrous tissue capsule was also evident demarcating the transplant area (Fig. 7c); however, this capsule was quite thin when compared with that seen in the control samples. In this sample, there is a combination of features consisting of numerous blood vessels surrounded by a dense cellular fibrous tissue and with a nearby homogeneous pink

patch, an organisation perhaps analogous to tissues of the dentine/pulp complex (Fig. 7d).

Other areas in the group II 2-week test samples, showed very large osteodentine-like patches with fine lace-like patterns at their periphery (Fig. 8a) with minute holes in a homogeneous pink matrix (Fig. 8b). Another interesting observation in this group of specimens is the presence of a characteristic vertical arrangement of columnar cells especially adjacent to the walls of the large blood vessels (Fig. 8c). Next to these cells are numerous fibroblast-like cells embedded in a dense collagen matrix. In some areas there are pink patches right next to these cellular arrangements (Fig. 8d).

For group I 6-week control samples, there was no sign of a fibrous tissue capsule. Instead, there is an area of dense fibrous tissue devoid of skin appendages which are present on either side of this area probably where the scaffold was implanted (Fig. 9a). This area could be gradually replacing the scar tissue seen in the 2-week samples. There is also a noticeable increase in vasculature seen upon higher magnification (Fig. 9b).

Upon the examination of the group I 6-week test specimens, a variety of different structures could be identified in these specimens just above the muscle layer (Fig. 9c). All of the structures noticed were surrounded by or in

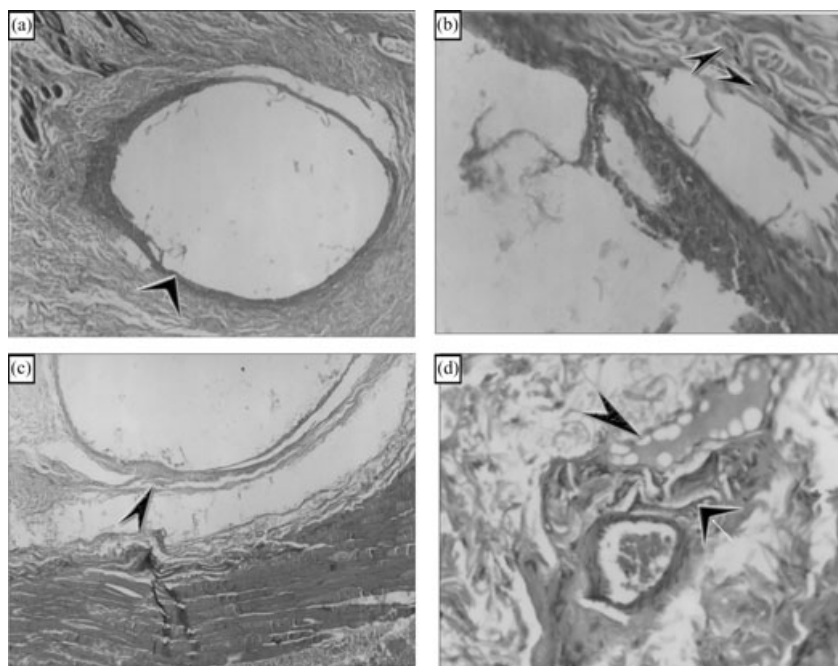


**Figure 7** Histological micrographs of group II implants – 2 weeks following transplantation (H&E). (a) Control sample (without cells) showing a fibrous tissue capsule surrounding area of implanted scaffold ( $\times 40$ ); (b) control sample (without cells) numerous budding capillaries related to the capsule wall ( $\times 200$ ); (c) test sample (with cells) showing a thin fibrous tissue capsule in the area where the scaffold was implanted ( $\times 40$ ); (d) test sample (with cells) showing an osteodentine-like patch (narrow arrowhead) and dense cellularity in surrounding area (wide arrowhead) ( $\times 200$ ).

close approximation to numerous newly forming blood vessels and budding capillaries (Fig. 9d). There were several well-circumscribed subcutaneous areas filled with homogeneous pink patches and in some other areas, these patches showed a banded appearance. These spaces were lined with flattened elongated cells in thin capsule-like boundaries. Some of these patches appeared interlacing with fine filament-like structures, which could be that the scaffold is degrading in accordance with a homogenous deposition of tissue. Some of these patches appeared very dense with minute holes in them giving a honey-comb-like appearance which may represent osteodentine (Fig. 9e,f). Around these structures, there is increased cellularity in the form of numerous stellate-shaped or fibroblast-like cells.

Another observation is the presence of cells in tubular-like arranged patterns, taking the appearance of a loop with dense cellularity and blood vessels in the immediate neighbouring area (Fig. 9g). Some of these tubular structures have well-arranged vertically aligned columnar cells with elongated nuclei, which may be odontoblast-like cells. These structures are surrounded by a thin capsule (Fig. 9h).

Group II 6-week control samples revealed the presence of a very thin small capsule that is probably the resolution of the more well-defined capsule seen at 2 weeks

(Fig. 10a). This capsule seems to contain fibrous tissue as if it is undergoing a filling replacement of the degraded scaffold (Fig. 10b).

For the final and last group of specimens, the 6-week test specimens of group II, there is a very thin lining remaining from the capsule that was present at 2 weeks. The surrounding tissue appears normal with normal skin appendages (Fig. 10c). In accordance with the structures seen in the previous group, there are columnar cells arranged in tubular-like structures. There are also well-circumscribed elongated structures consisting of organised vertically arranged parallel tubules similar to a dentine-like appearance (Fig. 10d).

## Discussion

Restoring lost tooth tissue will be with us for many years to come (16). Although tooth autotransplantation, allotransplantation and dental implants have existed for many years, they have never been totally satisfactory. Thus, the development of new methods of tooth replacement has become desirable (1,2).

Despite that clinical success rates of endodontic treatments can exceed 90% (17), many teeth are not given the opportunity to be saved by endodontic treatment and instead are extracted. Regenerative endodontic methods

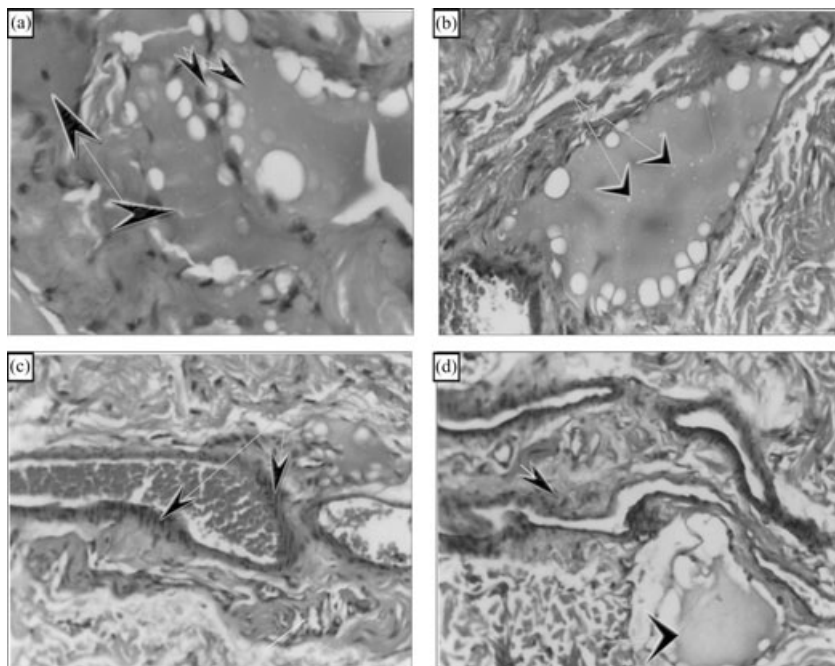


**Figure 8** Histological micrographs of group II test implants – 2 weeks following transplantation (H&E). (a) Test sample (with cells) showing osteodentine-like patches (arrowheads) with lace-like peripheries ( $\times 400$ ); (b) test sample (with cells) showing minute holes in the osteodentine-like patch (arrowheads) ( $\times 200$ ); (c) test sample (with cells) showing columnar-like arranged cells and dense cellularity around neighboring blood vessels (arrowheads) ( $\times 200$ ); (d) test sample (with cells) showing an osteodentine-like patch (wide arrowhead) and cellular arrangements (narrow arrowhead) with several blood vessels in the surrounding area ( $\times 200$ ).

have the potential for regenerating both pulp and dentine tissues and therefore may offer an alternative method to save teeth that may have compromised structural integrity (18).

By the emergence of this new terminology in endodontics, regenerative endodontics, it is then possible that one may start to contemplate the idea of biological tooth tissue substitutes that would perhaps adequately restore functional architecture found in normal physiological tissues.

In the present study, a tissue engineering concept was approached to explore the possibility of introducing regenerative procedures into the science of endodontics. Scaffolds with different features were used in the search for the optimal scaffold for dentine/pulp tissue regeneration, in addition to examining the unique features of dental pulp stem cells and their vast potential for regenerating dental tissues.

It has been suggested by several authors that optimal pore size of scaffolds for osteoconduction is between 100 and 350  $\mu\text{m}$  for regenerating bone (19,20). It is for this reason that the particle sizes chosen in the present work were within this range. The choice of varying the porosity criteria is simply due to the fact that there has not been focus on this area in the dental tissue engineering field.

Numerous scaffolds and drug delivery systems have been proposed with varying features (21), yet the scaffold choice and properties for dental tissue regeneration have not been explored in full (22–24).

In the current work, scaffolds prepared using the solvent-casting/particulate leaching technique from 50/50 PLGA showed relatively good porosity with good interconnecting pores for both groups attempted. The technique revealed a repeatable and dependable method of fabricating scaffolds for dental tissue engineering. It also allowed versatility in changing the parameters of design of the scaffold, regarding pore size, in order to achieve a scaffold with characteristics most suitable for this area of application. This indicates that this technique can be successfully used to tailor scaffolds with specific design characteristics: size, shape and porosity to be later on employed, for example, to the dimensions of a cavity preparation. Scanning electron microscopic analysis of the surface topography of the scaffolds showed a range of pores present on each scaffold and that these pores were interconnected throughout the bulk of the scaffold as evidenced by the appearance of smaller interconnecting pores within the larger surface pores.

From the surface characteristics, group II appeared to have greater surface porosity than group I despite the fact

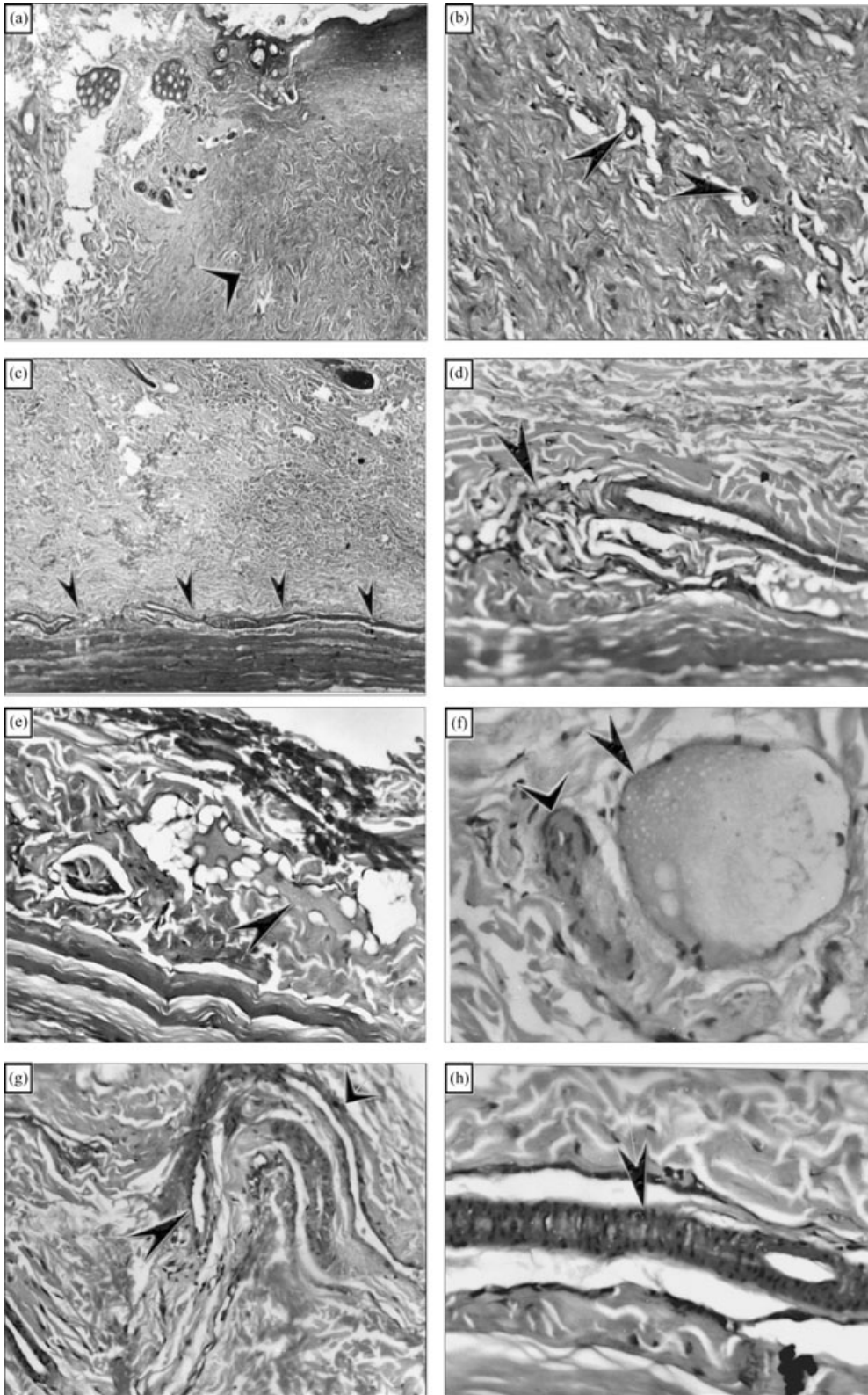


**Figure 9** Histological micrographs of group I implants – 6 weeks following transplantation (H&E). (a) Control sample (without cells) showing dense fibrous tissue at site of transplant (arrowhead) ( $\times 40$ ); (b) control sample (without cells) showing increased vasculature and budding capillaries at site of implant (arrowheads) ( $\times 200$ ); (c) test sample (with cells) showing a variety of regenerated structures above the muscle layer (arrowheads) ( $\times 40$ ); (d) test sample (with cells) showing homogeneous pink patches and budding capillaries (arrowhead) ( $\times 200$ ); (e) test sample (with cells) showing a homogeneous pink patch with foam-like borders (arrowhead) ( $\times 200$ ); (f) test sample (with cells) showing an osteodentine-like patch (narrow arrowhead) and numerous stellate-shaped cells surrounding it (wide arrowhead) ( $\times 200$ ); (g) test sample (with cells) showing well-organised loop-like arrangement of dense cells (wide arrowhead) and regenerated blood vessels in the vicinity (narrow arrowhead) ( $\times 400$ ); (h) test sample (with cells) showing a tubular structure with vertically aligned columnar cells (arrowhead) ( $\times 400$ ).

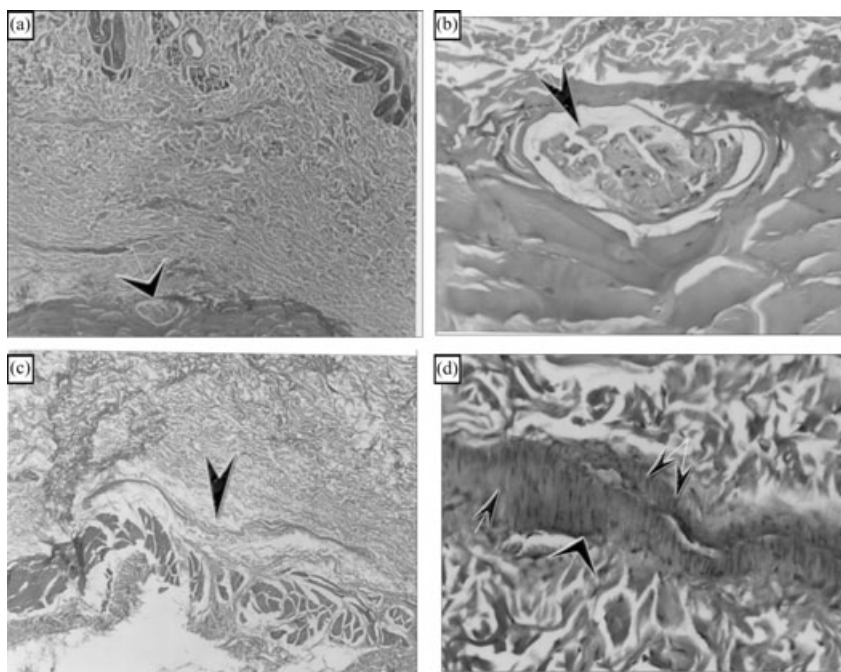


**Figure 10** Histological micrographs of group II implants – 6 weeks following transplantation (H&E). (a) Control sample (without cells), with arrowhead showing a fibrous tissue capsule in place of the implant ( $\times 40$ ); (b) control sample (without cells), arrowhead showing fibrous tissue filling in the remaining capsule ( $\times 200$ ); (c) test sample (with cells), arrowhead showing thin remnants of capsule in place of the degraded implant ( $\times 40$ ); (d) test sample (with cells), area showing tubular structures (wide arrowhead) having organised vertically arranged parallel tubules (narrow arrowheads) resembling a tubular-like dentine matrix ( $\times 200$ ).

that this group registered the least number of macropores and the least porosity percentage. This might be due to the fact that, when measuring porosity in these very thin films, the more porous the surface of the scaffold, the surface area of the top and bottom of the scaffolds in contact with the mercury may be included in the surrounding volume; hence, the recorded porosity may represent that, that is in the structure of the material without considering the surface pores. This is further concluded by the fact that group II data showed very few macropores although those were quite evident in the scanning electron micrographs.

Although there was an obvious difference between the groups as regards to pore size distribution, this difference did not seem to have an impact on the histological results.

For both groups, there was a distribution of small and large pores with varying degrees. These pores appeared to be sufficient in supporting cell growth for all of the groups attempted as shown by the infiltration of cell populations deep inside the pores (SEM). It is possible to predict that maintaining a large range of pore sizes in scaffolds used for dental tissue engineering will provide an important combination of several features needed to support the growth of a heterogeneous cell population (specialised and undifferentiated cells, blood cells, lymphatics, nerve cells) to give rise to a complicated and sophisticated tissue such as the dentine/pulp complex.

It might be possible that greater porosities with more macropores could support the formation of an osteodentine-like matrix, while scaffolds with less

porosity and much more micropores could support the formation of more organised matrix deposition more similar to dentine. It is also possible that due to the fact that the amount of osteodentine-like tissue was noticeably much more in group II test specimens especially at 2 weeks, this could have provided a large surface area for the attachment and differentiation of the dental pulp stem cells and so resulted in a more tubular dentine-like matrix by 6 weeks.

Another factor that should not be overlooked is the effect of biodegradation of the scaffolds on the porosity. Porosity has been shown to increase as the material degrades following the *in vivo* transplantation into the body. This results in the increase of average pore size and the appearance of bottlenecks in the continuity of the pore structure (20). This process may help boost the regeneration process by giving the cells more room to take over and secrete their own extracellular matrix, as well as providing channels for the escape of the biodegradation and waste products. As the newly forming tissue remodels into mature shape, the scaffold begins to disintegrate after performing its functions of mechanical support and cueing for the cells.

When examining the clinical potential of using cell-based tissue engineering for endodontic regenerative procedures, there are many supportive facts. As evidenced by the present study and in accordance with many others, dental pulp stem cells can provide an ample source for the regeneration of lost dentine and pulp tissues as well as other non-dental tissues (25,26). In the present study, dental pulp stem cells were easily isolated from rabbit teeth as they have been isolated from other species. These cells demonstrated high proliferation and clonogenic ability with typical fibroblast-like morphology as well as staining positive for the mesenchymal stem cell marker cd271 (7,9,27). When the dental pulp stem cells were cultured *in vitro* for prolonged periods, nodule-like structures formed on the bottom of the tissue culture flasks indicating dense extracellular matrix secretion and the possibility that the cells may have differentiated into odontoblast-like cells that have begun laying down a dentine matrix in an organised fashion.

The fact that dental pulp stem cells have the ability to differentiate into dentine-forming cells has been elucidated by many studies. However, in most of these experiments, the formation of mineralised structures *in vitro* was only evident following the addition of differentiation chemicals such as ascorbic acid, dexamethasone, and  $\beta$ -glycerophosphate or growth factors such as BMP-2 (6). This is in contrast to the phenomenon observed in the present study where the cells formed mineralised-like structures even without the addition of any motivating factors (10).

Furthermore, upon seeding the various types of scaffolds with isolated and cultured dental pulp stem cells and observing them over a period of 12 days, another phenomenon could be observed. For both groups, there were nodule-like structures with an organised nature that seemed to be distributed across the entire surface of the scaffolds showing that, not only were the cells capable of forming characteristic structures during *in vitro* culturing, but also when second or third passage cells were used to seed the scaffolds. This possibly means that the cells did not lose their characteristic inherent nature even after prolonged periods of culturing. The ability of dental pulp stem cells to deposit dense extracellular matrix in an organised fashion shows the specific nature of this population of stem cells, and the possibility that these cells may undergo differentiation into hard tissue forming cells when provided with the appropriate substrate.

Possibly the change in external environment could encourage the cells into differentiating into dentine-forming cells, hence providing us with a sufficient amount of tissue *ex vivo* which could be later transplanted to heal even an infected or inflamed dentine/pulp complex. It is perhaps possible that these tissue-residing progenitor cells are provided with other signalling mechanisms that elicit their differentiation *in vivo*. One author has stated that dentine matrix represents both an effective exogenous stimulus and an appropriate substrate for the direct induction of cytological and functional odontoblast-like cell differentiation (28).

Histological results showed that, a fibrous tissue capsule was found present in all but one of the 2-week control and test specimens; however, this capsule resolved by time and was absent in almost all of the 6-week samples. The absence of inflammatory cells in all of the samples studied, whether control or test, demonstrates the biocompatible nature of the transplants and favourable host reaction.

The increased vascularisation present in the control (Fig. 7b) as well as the test transplants (Fig. 8d) also emphasises the effect of the presence of the dental pulp stem cells coupled with the microporosity of the scaffold on neovascularisation which is an important aspect of any tissue regeneration regimen. This is especially important when dealing with a vascular tissue such as the dental pulp.

Numerous budding capillaries were proof of the effect of the scaffold microporosity on the new vascularity. Since micropores (5  $\mu$ m) are important to support neovascularisation, and larger pores are necessary to promote stem cell migration, proliferation and differentiation, as well as transport of nutrients and waste, the presence of a variety of small and large pores is desirable. A large surface area favours cell attachment and growth,

whereas a large pore volume is required to accommodate and subsequently deliver a cell mass sufficient for tissue repair (19,20).

In many instances, the characteristic homogeneous patches noticed microscopically were in close proximity to large blood vessels and newly forming capillaries (Fig. 9d,g). This possibly, again sheds light on the role of the dental pulp stem cells in supporting angiogenesis. Some of the patches also contained areas where there appeared to be some blood-derived cells, indicating that the process of hard tissue deposition and new tissue formation was going hand in hand together with the formation of new blood vessels.

During angiogenesis, endothelial cells migrate, proliferate, form a highly organised three-dimensional structure and produce a basement membrane until cell migration ceases. This structure could promote the process of pulp cell differentiation in the same manner as the basement membrane during odontogenesis. All of these factors are important as well as the possibility that the dental pulp stem cells themselves, besides being capable of differentiation, may also be able to induce host cells to participate in tissue regeneration by the formation of a pulp-like complex which could be seen in the present work in some of the 6-week test samples (27,29).

Despite the fact that teeth have been shown to mineralise in response to injury for many decades, only in recent years has the position of the stem cells been localised around blood vessels. The cells have been identified as myofibroblastoid pericytes (30). Based on recent studies in developmental biology, it has been suggested that a number of different stem cells may arise from developing blood vessels (7). It is possible that this partly explains the regeneration pattern seen in the present work accompanied by the formation of blood vessels and occurring almost always in their vicinity, as well as the presence of some combination structures (Fig. 7d).

The formation of patches of osteodentine-like matrix in the present work as early as 2 weeks post transplantation (Fig. 8a,b), shows the promising nature of using a tissue engineering approach to regenerate more repair tissue at shorter time intervals than those required for instance, for vital pulp therapy. In many instances, these patches had the appearance of osteodentine and were lined with flattened cells that may be stem cells that have become differentiated into osteodentineoblasts and have begun secreting a hard tissue matrix (Fig. 9f). Osteodentine may serve as the substrate for the attachment of odontoblast-like cells which would then begin secreting tubular dentine. It has been shown by several authors that the formation of an atubular fibrodentine or osteodentine matrix is a precursor to the formation of a more organised tubular matrix (6,31,32). In other instances in the current

study, these patches appeared denser and had characteristic striations.

The appearance of more organised structures in the test specimens, which were lined by several layers of cells possibly, denotes that the dental pulp stem cells have begun to differentiate into characteristic odontoblast-like cells which have started to line up prior to secretion of extracellular matrix (Fig. 9h). Furthermore, in group II 6-week test specimens, some of these structures showed columnar well-arranged cells surrounding large blood vessels (Fig. 8c) and at the same time present next to some of the homogeneous patches described before. These areas appeared to be surrounded by densely cellular fibrous tissue perhaps reminiscent of the appearance of a dentine/pulp-like complex. This again reflects the possibility that dental pulp stem cells are differentiating into hard tissue forming cells and at the same time inducing host tissues to contribute to the formation of a pulp-like tissue (27).

More significant changes were seen in the 6-week samples as they represented a longer term for evaluation of the effects of the transplanted constructs. In most of the 6-week test specimens, many of the structures seen in the 2-week test samples were again present. These however appeared to occur more frequently and over larger surface areas. Some of the 6-week specimens, however, revealed characteristic structures that did not seem to present in all of the 2-week test specimens. It is significant that in some instances especially in group I 6-week test specimens, some of these structures began to assume a loop-like appearance perhaps similar to the layers present in a natural tooth (Fig. 9g). This has been previously demonstrated by several studies following the transplantation of dental pulp stem cells with a hydroxyapatite/tricalcium phosphate (HA/TCP) matrix subcutaneously, where the formation of highly organised dentine/pulp complex could be seen. However, despite the similarity of the results of the present study to that work, tissues regenerated here appeared less organised. This is possibly due to the difference in the matrix used, as HA/TCP is a known osteoconductive substance, the authors suggest that it may also be odontoconductive which may explain this difference (9,27,33).

Furthermore, 6-week test specimens showed tubular bilayered structures of vertically aligned parallel tubules that may represent the formation of a tubular-like dentine (Fig. 10d). Again, these observations support the fact that the dental pulp stem cells had undergone differentiation into odontoblast-like cells which utilised the osteodentine-like matrix for attachment and secretion of a more tubular dentine-like matrix. This is also coupled with the presence of a wide range of pore sizes present in the scaffold to support the regeneration of such a heterogeneous tissue such as the dentine/pulp complex.

## Conclusions

It can be concluded that using a PLG scaffold with specially designed characteristics may act as a suitable matrix to support dental pulp stem cells and their differentiation to form an organised dentine/pulp-like tissue. Controlling pore size obviously has great impact on the nature of the regenerated tissues. Although larger pore sizes closer to 300  $\mu\text{m}$  may support a substantial amount of regenerated mineralised tissues, maybe smaller pore sizes by providing a matrix for angiogenesis will allow the regeneration of more organised tissues. Perhaps the optimum scaffold is one which combines a large range of pore sizes which will combine both advantages. It is also important not to overlook the increase in porosity and change in pore size that accompanies the degradation of the scaffold.

It is also obvious that the amount of regenerated tissue increased as the time interval of the experiment increased. However, the spatial organisation of the regenerated tissues in this study was not explained. In some areas, the tissues appeared well-organised while in other areas they did not. However, the frequency of organised tissue formation did increase with time. The range of characteristics of these newly formed tissues may perhaps be more controlled if extrinsic bioactive molecules are added to the cell/scaffold construct, and their effects explored in a separate study.

Finally, results from the present work managed to display the capacity of using a tissue engineering concept to regenerate a variety of dentine-like and pulp-like tissues. The regenerated tissues appeared to be quite similar to well-known repair tissues seen in *in vivo in situ* situations. This indicates that tissues regenerated by tissue engineering can closely simulate those that are formed by naturally occurring events.

Advancement in the understanding of tooth development in molecular biology as well as cell biology has set a stage for the efforts to develop strategies for regenerating tooth organs. Recent reports on the engineering of dental tissues using different cell sources suggest the potential of bioengineering strategies for tooth regeneration (34,35). The major challenge herein is to achieve the complete and controlled spatial growth of tooth complex, with appropriate size, morphology and functional aspects (34,36). It is by combining the collective knowledge of developmental sciences with the vast arena of clinical research will the true potential of these new therapies be achieved.

## Acknowledgements

This work was funded in part by The Academy of Scientific Research and Technology, Egypt and so the authors

duly acknowledge their support. The authors would also like to acknowledge the help of the entire team at the Tissue Engineering Laboratories, Faculty of Dentistry, Alexandria University, Egypt.

## References

1. Nakashima M, Akamine A. The application of tissue engineering to regeneration of pulp and dentin in endodontics. *J Endod* 2005; 31: 711–8.
2. Yen A, Sharpe P. Regeneration of teeth using stem cell-based tissue engineering. *Expert Opin Biol Ther* 2006; 6: 9–16.
3. Tziafas D, Smith AJ, Lesot H. Designing new treatment strategies in vital pulp therapy. *J Dent* 2000; 28: 77–92.
4. Atala A, Lanza RP. *Methods of tissue engineering*. San Diego, CA: Academic Press; 2002.
5. Young CS, Terada S, Vacanti JP, Honda M, Bartlett JD, Yelick PC. Tissue engineering of complex tooth structures on biodegradable polymer scaffolds. *J Dent Res* 2002; 81: 695–700.
6. Iohara K, Nakashima M, Ito M, Ishikawa M, Nakasima A, Akamine A. Dentin regeneration by dental pulp stem cell therapy with recombinant human bone morphogenetic protein 2. *J Dent Res* 2004; 83: 590–5.
7. Gronthos S, Mankani M, Brahimi J, Robey PG, Shi S. Postnatal human dental pulp stem cells (DPSCs) in vitro and in vivo. *PNAS* 2000; 97: 13625–30.
8. Gronthos S, Brahimi J, Li W *et al.* Stem cell properties of human dental pulp stem cells. *J Dent Res* 2002; 81: 531–5.
9. Miura M, Gronthos S, Zhao M, Lu B, Fisher LW, Robey PG, Shi S. SHED: stem cells from human exfoliated deciduous teeth. *PNAS* 2003; 100: 5807–12.
10. Zhang W, Walboomers XF, Wolke JGC, Bian Z, Fan MW, Jansen JA. Differentiation ability of rat postnatal dental pulp cells in vitro. *Tissue Eng* 2005; 11: 357–68.
11. Sonoyama W, Liu Y, Fang D *et al.* Mesenchymal stem cell-mediated functional tooth regeneration in swine. *PLoS ONE* 2006; 1: e79. doi:10.1371/journal.pone.0000079.
12. Aj S, Goldberg M. Cells and extracellular matrices of dentin and pulp: a biological basis for repair and tissue engineering. *Crit Rev Oral Biol Med* 2004; 15: 13–27.
13. Morgan JR, Yarmush ML. *Tissue engineering methods and protocols*. Totowa, NJ: Human Press Inc; 1999.
14. Mikos AG, Temenoff JS. Formation of highly porous biodegradable scaffolds for tissue engineering. *Electron J Biotechnol* 2000; 3: 114–9.
15. Webb PA. An introduction to the physical characterization of materials by mercury intrusion porosimetry with emphasis on reduction and presentation of experimental data. Norcross, GA: Micromeritics Instrument; 2001.
16. Smith AJ. Tooth tissue engineering and regeneration – a translational vision! *J Dent Res* 2004; 83: 517.

17. Friedman S, Mor C. The success of endodontic therapy: healing and functionality. *J Calif Dent Assoc* 2004; 32: 493–503.
18. Murray PE, Garcia-Godoy F, Hargreaves KM. Regenerative endodontics: a review of current status and a call for action. *JOE* 2007; 33: 377–90.
19. Whang K, Healy KE, Elenz DR, Chua CK. Engineering bone regeneration with bioabsorbable scaffolds with novel microarchitecture. *Tissue Eng* 1999; 5: 35–51.
20. Yang S, Leong K, Du Z *et al.* The design of scaffolds for use in tissue engineering. Part I. Traditional factors. *Tissue Eng* 2001; 7: 679–89.
21. Wang FM, Qiu K, Hu T, Wan CX *et al.* Biodegradable porous calcium polyphosphate scaffolds for the three-dimensional culture of dental pulp cells. *IEJ* 2006; 39: 477–83.
22. Muioli EK, Clark PA, Xin X, Lal SH, Mao JJ. Matrices and scaffolds for drug delivery in dental, oral and craniofacial tissue engineering. *Adv Drug Deliv Rev* 2007; 59: 308–24.
23. Buurma B, Gu K, Rutherford RB. Transplantation of human pulpal and gingival fibroblasts attached to synthetic scaffolds. *Eur J Oral Sci* 1999; 107: 282–9.
24. Bohl KS, Shon J, Rutherford B, Mooney DJ. Role of synthetic extracellular matrix in development of engineered dental pulp. *J Biomater Sci Polym Ed* 1998; 9: 749–64.
25. Zhang W, Walboomers XF, van Kuppevelt TH, Daamen WF, Bian Z, Jansen JA. The performance of human dental pulp stem cells on different three-dimensional scaffold materials. *Biomaterials* 2006; 27: 5658–68. Epub 2006 Aug 17.
26. d'Aquino R, Papaccio G, Laino G, Graziano A. Dental pulp stem cells: a promising tool for bone regeneration. *Stem Cell Rev* 2008; [Epub ahead of print].
27. Batouli S, Miura M, Brahim J *et al.* Comparison of stem-cell-mediated osteogenesis and odontogenesis. *J Dent Res* 2003; 82: 976–81.
28. Tziafas D, Belibasakis G, Veis A, Papadimitriou S. Dentine regeneration in vital pulp therapy: design principles. *Adv Dent Res* 2001; 15: 96–100.
29. Magloire H, Joffre A, Bleicher F. An in-vitro model of human dental pulp repair. *J Dent Res* 1996; 75: 1971–8.
30. Murray PE, Garcia-Godoy F. Stem cell responses in tooth regeneration. *Stem cells Dev* 2004; 13: 255–62.
31. Tziafas D. Dentinogenesis in the traumatized pulp. In: Tziafas D, ed. *Reparative dentinogenesis: a monograph on the dentinogenic potential of dental pulp*. Thessaloniki: University Studio Press; 1997. pp. 45–9.
32. Yoshida K, Yoshida N, Nakamura H, Iwaku M, Ozawa H. Immunolocalization of fibronectin during reparative dentinogenesis in human teeth after pulp capping with calcium hydroxide. *J Dent Res* 1996; 75: 1590–97.
33. Mooney DJ, Powell C, Piana J, Rutherford B. Engineering dental pulp-like tissue in vitro. *Biotechnol Prog* 1996; 12: 865–68.
34. Mikos AJ, Herring SH, Ochareon P *et al.* Engineering complex tissues. *Tissue Eng* 2006; 12: 3307–39.
35. Ferreira CF, Magini CS, Sharpe PT. Biological tooth replacement and repair. *J Oral Rehabil* 2007; 34: 933–9.
36. Du C, Moradian-Oldak J. Tooth regeneration: challenges and opportunities for biomedical material research. *Biomed Mater* 2006; 1: 10–17.